Altered mechanical interaction between rat plantar flexors due to changes in intermuscular connectivity

Bernabei, M.; van Dieen, J.H.; Maas, H.

published in
Scandinavian Journal of Medicine and Science in Sports
2016

DOI (link to publisher)
10.1111/sms.12644

Scand J Med Sci Sports 2017: 27: 177–187
doi: 10.1111/sms.12644

SCANDINAVIAN JOURNAL OF
MEDICINE & SCIENCE
IN SPORTS

Altered mechanical interaction between rat plantar flexors due to changes in intermuscular connectivity

M. Bernabei, J. H. van Dieën, H. Maas

Department of Human Movement Sciences, Vrije Universiteit Amsterdam, MOVE Research Institute Amsterdam, Amsterdam, The Netherlands
Corresponding author: Huub Maas, Van der Boechorststraat 9, 1081 Amsterdam, The Netherlands. Tel.: +31 20 59 82568, Fax: 020-5988529, E-mail: h.maas@vu.nl

Accepted for publication 2 December 2015

Connective tissue formation following muscle injury and remedial surgery may involve changes in the stiffness and configuration of the connective tissues linking adjacent muscles. We investigated changes in mechanical interaction of muscles by implanting either a tissue-integrating mesh (n = 8) or an adhesion barrier (n = 8) to respectively increase or decrease the intermuscular connectivity between soleus muscle (SO) and the lateral gastrocnemius and plantaris complex (LG+PL) of the rat. As a measure of mechanical interaction, changes in SO tendon forces and proximal–distal LG+PL force differences in response to lengthening LG+PL proximally were assessed 1 and 2 weeks post-surgery. The extent of mechanical interaction was doubled 1 week post-implantation of the tissue-integrating mesh compared to an unaffected compartment (n = 8), and was more than four times higher 2 weeks post-surgery. This was found only for maximally activated muscles, but not when passive. Implanting the adhesion barrier did not result in a reduction of the mechanical interaction between these muscles. Our findings indicate that the ratio of force transmitted via myofascial, rather than myotendinous pathways, can increase substantially when the connectivity between muscles is enhanced. This improves our understanding of the consequences of connective tissue formation at the muscle boundary on skeletal muscle function.

A number of *in situ* experiments in animals (for a review, see Huijing, 2009) and imaging studies in humans (Bojsen-Moller et al., 2010; Huijing et al., 2011; Tian et al., 2012; Yaman et al., 2013) have shown that intermuscular and extramuscular myofascial connective tissues can serve as a pathway for force transmission. Effects of epimuscular myofascial pathways may be enhanced in pathological conditions of the musculo-skeletal system in which the properties of connective tissues linkages have been altered (Maas & Sandercock, 2010). If such connections are either stiffer or more compliant than normal, resultant changes in the magnitude of intermuscularly transmitted forces may have significant effects on muscle mechanics (Smeulders & Kreulen, 2007; Yucesoy & Huijing, 2007; Huijing et al., 2010).

Scar tissue formation in response to muscle and tendon injuries may increase the stiffness of intermuscular connections. Animal studies have suggested that scar tissue formation observed post-surgery may explain the frequent recurrence of injury to strained muscles (Nikolaou et al., 1986; Garrett et al., 1988). Also, a reduction of the overall muscle belly displacement and a localized increase of tissue strain has been associated with the presence of scar tissue following hamstring injury in humans (Silder et al., 2008, 2010). Given the continuity between the intramuscular and extramuscular connective tissues, such within muscle effects could translate into an increase of mechanical interactions between muscles. Enhanced interactions between synergists may result also from muscle–tendon–bone interventions and remedial surgeries (e.g., tendon transfers). In fact, inter- and extramuscular connective tissues are commonly dissected in those interventions, assuming that a muscle output is independent of adjacent structures. In contrast, *in situ* experiments in rats (Maas & Huijing, 2012a,b; Maas et al., 2013), finite element modeling (Yucesoy & Huijing, 2007), and studies on cerebral palsy patients (Kreulen et al., 2003; Smeulders et al., 2005) have shown that clinical outcomes of surgical procedures such as aponeurotomy, tenotomy, and tendon transfers depend on the degree of connectivity between the target muscle and neighboring synergists. Instead of increased stiffness, other pathological conditions involve more compliant connective tissues. Using a tenascin-X-deficient mouse, a

model of Ehlers-Danlos syndrome, it was shown that such increased compliance significantly reduces the extent of mechanical interaction between adjacent muscles (Huijing et al., 2010).

The animal studies described above applied muscle lengths and relative positions beyond those found during normal movements of the corresponding joints. Moreover, direct assessment of mechanical interactions between muscles in humans requires invasive approaches (Smeulders et al., 2004), which are not suitable for healthy controls and do not provide evidence regarding the consequences on muscle mechanical function after recovery from the surgical intervention. Due to these limitations, the effects of changes in muscle connectivity as a result of injury, intervention, or disease on force transmission between adjacent muscles are still unclear.

The aim of the present work was to investigate the effects of changes in intermuscular connectivity on the mechanical interactions between rat ankle plantar flexors for physiological muscle lengths and relative positions. A local increase or decrease in the amount of intermuscular connective tissue was induced by implanting either a tissue-integrating mesh or an adhesion barrier mesh at the interface between soleus (SO) muscle and the complex of lateral gastrocnemius and plantaris muscles (LG+PL). We hypothesized that these mesh implantations will result in an increase or a decrease, respectively, of mechanical interactions between the ankle plantar flexion muscles.

Methods

Animals

Adult male Wistar rats ($n = 24$; mean ± SD body mass: 311.6 ± 13.3 g, Table 1) were randomly assigned to one of the three groups. Eight rats in the intact group (control) and eight rats in each of the two connectivity-manipulated groups (tissue-integrating mesh group, TI; adhesion barrier group, AB). The latter groups were each tested 1 ($n = 4$) and 2 weeks ($n = 4$) after the connectivity manipulation surgery. Surgical and experimental procedures were approved by the Committee on the Ethics of Animal Experimentation at the VU University Amsterdam and in strict agreement with the guidelines and regulations concerning animal welfare and experimentation set forth by Dutch law.

Table 1. Animal and muscle sizes in the operated and non-operated groups (mean ± SD)

Groups	Animal size (g)	SO muscle mass (g)	SO+LG+PL muscle mass (g)
Control	311.1 ± 4.5	0.20 ± 0.02	1.60 ± 0.16
TI (1 week)	312.3 ± 12.4	0.18 ± 0.02	1.67 ± 0.21
TI (2 weeks)	301.0 ± 18.8	0.19 ± 0.03	1.67 ± 0.13
AB (1 week)	304.8 ± 6.3	0.20 ± 0.03	1.60 ± 0.12
AB (2 weeks)	330.0 ± 10.2*	0.24 ± 0.05	1.79 ± 0.19

*$P = 0.002$, Bonferroni adjustment for multiple comparisons.

Surgical procedures for intermuscular connectivity manipulation

A one-time pre-operative subcutaneous injection of a painkiller (0.02 mg/kg, Temgesic®, Schering-Plough, Maarssen, The Netherlands) was administered to prevent discomfort of the animal following the survival surgery. Additional doses were given 1–2 days after the surgery if signs of pain were noticed. Following preparation for aseptic surgery and inhalation anesthesia (2–3% isoflurane), a skin incision was made on the dorsal side of the left lower leg to expose the lateral side of the posterior crural compartment. In the rat, the posterior and accessory heads of the biceps femoris insert with a common tendinous sheath into the distal end of the femur and the proximal two-thirds of the tibia (Greene 1935). A partial resection of this sheath was performed to access the compartment of SO and LG+PL muscles. The incision was performed parallel to the tibia and attention was paid to minimize damage to the biceps femoris myofibers. The lateral side of the posterior crural compartment was accessed by a partial fasciotomy of the surrounding crural fascia, limiting the exposure of the posterior crural muscles to the proximal two-thirds of the SO and LG muscle–tendon units (MTU). The distal portion of the biceps (accessory head) and posterior crural fascia, covering the distal myotendinous junctions of SO, LG, medial gastrocnemius, and PL as well as the Achilles tendon, were left intact. Myofascial linkages between the dorsal side of the SO and the ventral side of LG+PL were removed by blunt dissection and either an anti-adhesion barrier ($n = 8$; Physiomesh™; Ethicon, Norderstedt, Germany) or a tissue-integrating mesh ($n = 8$; Premilene® mesh; B. Braun Melsungen AG, Germany) was implanted at the interface of SO and LG+PL muscles. Attention was paid to prevent damage of the SO neurovascular tract, which runs centrally between SO and LG muscle bellies. A small opening in the central region of the mesh was made to avoid contact with this tract (Fig. 1B). The anti-adhesion barrier is composed by a double layer of absorbable poliglecaprone-25 suture polymer, which is the actual tissue separating layer that prevents adhesions during healing, and an inner flexible, macroporous mesh made of polypropylene which provides structural support. The tissue-integrating mesh consists of monofilament polypropylene knitted in a monolayer flexible mesh. These surgical meshes were originally designed for various interventions of hernia or chest repair to support the abdominal wall (Novitsky et al., 2007; Rodríguez et al., 2011).

Surgical procedures for *in situ* experiments

The surgical procedures and the experimental setup for the *in situ* measurements have been described elsewhere (Bernabei et al., 2015). Briefly, following an intraperitoneal injection of urethane solution (1.2 mL/100 g body mass, 12.5% urethane solution), the posterior crural compartment was exposed by removing the left hindlimb skin, biceps femoris, and medial gastrocnemius muscles. The SO, LG, and PL muscle group was dissected free from surrounding structures, preserving the bone insertions, as well as the myofascial connections at the interface between the SO and LG+PL muscle bellies. The distal tendon of SO was carefully dissected free from the rest of the Achilles tendon. Kevlar wires were used to connect the proximal and distal tendons of LG+PL as well as the distal tendon of SO to force transducers (Fig. 1A), which were positioned in such a way that forces could be measured in the muscle's line of pull, and that the relative position of muscles and tendons mimicked those present during normal movements. A tight knot was placed on the tendons prior to severing them

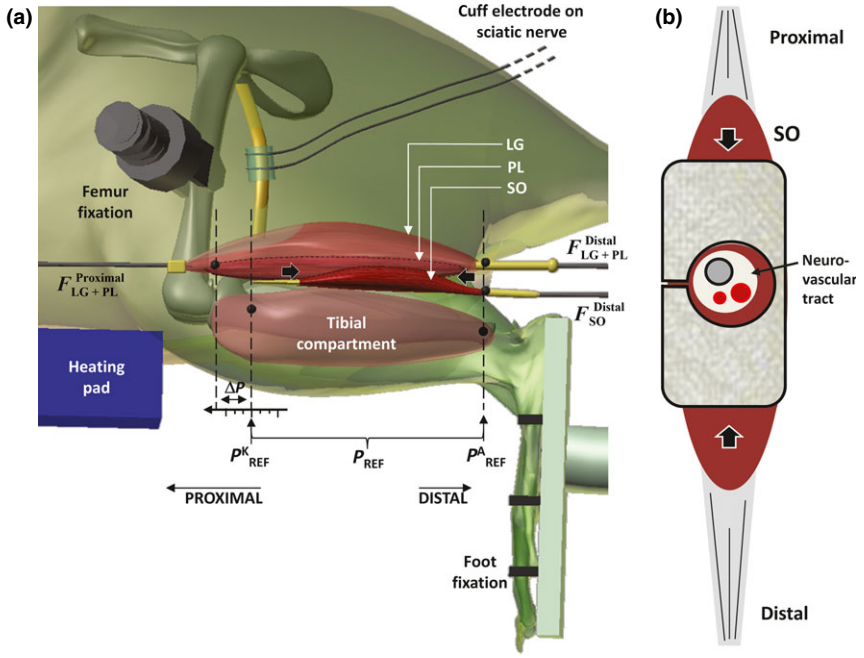

Fig. 1. Schematic of the experimental setup. (a) Lateral view of the rat left hindlimb in the experimental setup. Proximal and distal tendons of LG+PL as well as the distal tendon of SO were connected to separate force transducers. The femur was fixed with a metal clamp, the foot with a plastic plate. A bipolar cuff electrode was placed on the sciatic nerve. The five reference markers (black dots) applied on the tendons and on the anterior tibial compartment identified the reference position (P_{REF}), i.e., the MTU length corresponding to a 90°–90° knee–ankle joint configuration. ΔP describes the applied positional changes for proximal LG+PL tendon (−3 to +3 mm corresponding to 45° to 130° knee extension) with the distal SO and LG+PL tendons kept at (corresponding to 90° ankle angle). (b) Schematic representation of the surgical mesh shape and position. The anti-adhesion barrier or the tissue-integrating mesh was implanted at the interface of the synergistic SO and LG+PL muscles after blunt dissection of the myofascial connective tissues. A small opening in the central region of the mesh was made to avoid contact with SO neurovascular tract. Thick black arrows in (a) and (b) indicate the implantation area.

from the skeleton to limit any relative sliding within the tendon. The rat was mounted in the experimental setup by clamping the femur and the foot such that knee and ankle joints were kept at 90°, which was defined as the *reference position* (P_{REF}). Markers were placed near the SO distal and LG+PL proximal and distal myotendinous junctions (Fig. 1), to identify the position of the distal tendons corresponding to P_{REF} for the ankle angle at 90° ($\boldsymbol{P^{A}_{REF}}$), the position of the LG+PL proximal tendon corresponding to P_{REF} for the knee angle at 90° ($\boldsymbol{P^{K}_{REF}}$) and to apply MTU length changes relative to the reference positions (ΔP). At the end of the measurements, the animals were euthanized with a pentobarbital (Euthasol 20%) overdose injected intracardially, followed by double-sided pneumothorax.

Nerve stimulation

SO and LG+PL were excited simultaneously via supramaximal stimulation of the tibial nerve (0.4 ± 0.1 mA, 500 ms, 100 Hz). Three twitches were evoked 1.5 s and 1 s before each tetanic stimulation, and 0.5 s after cessation of tetanic stimulation. Muscles were allowed to recover for 2 min between subsequent stimulations.

Experimental protocol

Prior to data collection, multiple contractions at high and low lengths were performed in order to prevent history effects. Isometric forces exerted at all three tendons were measured simultaneously for different lengths and relative positions of LG+PL and SO muscles. The proximal LG+PL tendon was repositioned in steps of 1 mm from $\boldsymbol{P^{K}_{REF}}$−3 mm, corresponding to ~45° knee angle, to $\boldsymbol{P^{K}_{REF}}$+3 mm, corresponding to ~130° knee angle (Johnson et al., 2008). The distal tendons of SO and LG+PL were kept at P_{REF}, so that MTU length of SO was constant. The range of imposed MTU lengths and relative positions were selected based on ankle and knee joint angles observed during normal movements, such as walking, swimming, ladder walking, and trotting (Gillis & Biewener, 2001; Canu & Garnier, 2009; Magnuson et al., 2009; Bauman & Chang, 2010).

Assessment of myofascial connections

Dissection was performed at the end of the *in situ* measurement to evaluate the location and characteristics of the newly grown myofascial connections at the synergists' interface. The actual location, integration (TI group), or absorption (AB group) of the surgical mesh was evaluated for those animals with manipulation of connectivity. Finally, individual muscles were harvested and weighted to identify changes in muscle mass between the intact and manipulated groups (Table 1).

Data analysis

Isometric forces were assessed from the force–time series: passive force (F_P) was assessed by calculating the mean over a 50 ms time window before the tetanic contraction and total

force was assessed by calculating the mean over the 50 ms before the end of the tetanic stimulation. LG+PL MTU lengths were expressed as the deviation (ΔP_{LG+PL}) from the length at P_{REF}. Two estimates of intermuscular mechanical interaction were assessed in this study: with repositioning of only the proximal LG+PL tendon over the full range, we measured (a) changes in force exerted at the distal tendon of SO (ΔF_{SO}), with SO kept at a constant length and (b) changes in the force difference between the proximal and distal tendons of LG+PL. The LG+PL force difference (ΔF_{LG+PL}) was calculated by subtracting the force exerted distally from the force exerted proximally (i.e., $F_{PROXIMAL} - F_{DISTAL}$), so that a positive difference indicates a higher proximal force. This force difference is a direct measure of the magnitude of net epimuscular myofascial force transmission (Huijing, 2009; Maas & Sandercock, 2010), which can be assessed at each imposed muscle length and relative position.

Assuming that myofascial pathways will carry forces between SO and LG+PL, a portion of the force produced by LG+PL myofibers is transmitted to the distal SO tendon and vice versa. To obtain force equilibrium, both ΔF_{SO} and $\Delta F_{PROX\text{-}DIST}$ would have to covary, as a function of the synergists' relative position ΔP. It should be noted that the neurovascular tracts of SO and LG+PL were intact. Via these tracts force can be transmitted to other structures than the synergistic group (Maas et al. 2003). Therefore, an exact complementary change of ΔF_{SO} and $\Delta F_{PROX\text{-}DIST}$ was not expected. Because the investigated muscles were almost fully isolated from their surroundings and the surgical manipulation affects only the myofascial connections at the SO and LG+PL interface, variations of ΔF_{SO} and $\Delta F_{PROX\text{-}DIST}$ were regarded as estimates of mechanical interaction between SO and LG+PL. In addition, LG+PL neutral position, defined as the LG+PL proximal tendon position yielding a zero LG+PL proximal–distal passive force difference, was calculated.

A preliminary comparison of the muscle masses showed no decrease of SO ($P = 0.100$) or SO+LG+PL ($P = 0.257$) muscle mass (Table 1). A difference in animals' body mass was found only between the control and AB group measured 2 weeks post-surgery (6.1% difference, $P = 0.02$). Total forces in the manipulated groups were substantially lower than in the controls, suggesting a change in force producing capacity of these muscles as a result of the mesh implantation surgery. To provide a fair comparison between groups, ΔF_{SO} and $\Delta F_{PROX\text{-}DIST}$ were normalized to the sum of the SO+LG+PL total force exerted distally ($F^{REF}_{SO+LG+PL}$) at P_{REF} (Table 2), and not to the forces exerted by the corresponding muscles. $F^{REF}_{SO+LG+PL}$ was selected as a normalization factor because we expected force transmission between the muscles and, thus, individual tendon forces do not originate exclusively from myofibers of the corresponding muscle belly. As muscle forces are redistributed among the distal tendons, the sum was considered as a valid measure of the overall force capacity of the synergistic group. Because no significant differences were found in SO and LG+PL passive forces, these data were not subjected to normalization.

As ΔF_{SO} and $\Delta F_{PROX\text{-}DIST}$ increased in a rather linear fashion with proximal lengthening of LG+PL for all tested groups, the force increase within the full range of applied LG+PL proximal positions was used as an overall estimate of mechanical interaction. Thus, the amount of mechanical interaction, described by the slope ($SLOPE$) of the ΔF_{SO} and $\Delta F_{PROX\text{-}DIST}$ curves, was assessed as follows:

$$\mathrm{SLOPE}_m = \frac{\Delta F_m(\Delta P_{\mathrm{range}})}{F^{REF}_{SO+LG+PL} \cdot \Delta P_{\mathrm{range}}} \quad (1)$$

where m represents the muscle considered, $\Delta P_{\mathrm{range}}$ is the full range of LG+PL proximal tendon positions (6 mm) applied and ΔF_m is either the amount of SO distal force increase (ΔF_{SO}) or the amount of the increase of LG+PL proximal–distal force difference ($\Delta F_{PROX\text{-}DIST}$) over $\Delta P_{\mathrm{range}}$. As the slope expresses the change in normalized force relative to the overall synergists' force producing capacity, it will not be affected by differential changes in muscle force capacity.

Statistics

ANOVA for repeated measures (within-subjects factor: LG+PL proximal tendon position, between-subjects factor: *group*) was used to test for changes in non-normalized passive and total forces of SO and LG+PL as well as for interaction effects (SPSS Statistics 20; IBM Corporation, Armonk, New York, USA). When a significant main effect was found ($P < 0.05$), Games–Howell post-hoc pairwise comparisons (specifically suitable when sample sizes are unequal and population variances differ) were used to test for individual group differences. Univariate ANOVAs (factor: group) were performed to test for changes in LG+PL neutral position, passive LG+PL force difference at P_{REF}, muscle and animal masses. In addition, regression analysis was used to evaluate covariation of $\Delta F_{PROX\text{-}DIST}$ and F_{SO} from P_{REF} −3 to P_{REF} +3 mm.

If ANOVA indicated a significant interaction effect, regression analysis for repeated measures using generalized estimating equations (GEE) was used to test for significant differences in mechanical interaction between groups (control, TI, AB). Normalized values of ΔF_{SO} ($SLOPE_{SO}$) and $\Delta F_{PROX\text{-}DIST}$ ($SLOPE_{LG+PL}$) were described as a function of the within-subject factor LG+PL proximal tendon position. A linear model was used, including interactions with the factor *group* to test whether the $SLOPE_{SO}$ and $SLOPE_{LG+PL}$ changed differently between groups. A first model considering the factor *manipulation* was used to compare TI ($n = 8$) and AB ($n = 8$) groups with the control ($n = 8$). Control animals were considered as the reference. A second model considering the factor *post-surgical recovery* allowed to test for differences between the TI and AB groups after 1 and 2 weeks after surgery [TI (1 week), TI (2 weeks), AB (1 week), AB (2 weeks): $n = 4$)]. In the latter, TI (1 week) and AB (1 week) groups were considered as the reference. For each non-redundant parameter, chi-square statistics were used to test for significance of estimates

Table 2. Muscle forces at REF length and values used for normalization in group comparisons (mean ± SD)

Groups	SO distal total force (N)	LG+PL proximal total force (N)	LG+PL distal total force (N)	Normalization factors (N)
Control	1.36 ± 0.08	11.45 ± 1.74	11.54 ± 1.78	12.90
TI (1 week)	1.01 ± 0.21	10.61 ± 1.67	10.46 ± 1.85	11.47
TI (2 weeks)	0.98 ± 0.26	7.31 ± 3.08	7.19 ± 2.95	8.17
AB (1 week)	0.59 ± 0.09	9.16 ± 1.67	9.16 ± 1.56	9.76
AB (2 weeks)	0.74 ± 0.24	7.83 ± 1.98	7.86 ± 2.03	8.60

between groups ($P < 0.05$). GEE was preferred to ANOVA for testing the effects of LG+PL position on total ΔF_{SO} and $\Delta F_{PROX\text{-}DIST}$ as the former allowed to consider LG+PL changes in length as a continuous, rather than a categorical variable. Therefore, the GEE is more appropriate to test for differences in mechanical interaction between groups.

Results

Intermuscular tissue remodeling

Exposure of the LG+PL and SO interface revealed substantial remodeling of the connective tissues. In the group with the tissue-integrating mesh, new intermuscular linkages were observed both proximally and distally with respect to the neurovascular tract of SO. In contrast to that of controls, the neurovascular tract itself was characterized by a compact bundle of connective tissue in which blood vessels and nerves were deeply embedded and no longer visible. In addition, the posterior crural fascia surrounding the ankle plantar flexors was denser than normal. Finally, separation of LG+PL and SO muscle bellies at the end of the *in situ* experiment revealed a partial or full integration of the implanted mesh by newly formed connective tissues.

Following implantation of the adhesion barrier, remodeling of the connective tissues linking SO and LG+PL was minimal. Exclusively areolar connective tissue was found 1 week post-surgery, mainly in the distal region of SO and LG+PL interface. Two weeks post-surgery, the adhesion barrier was partially degraded and newly formed connective tissue bundles were running between the muscle bellies.

Effects of LG+PL proximal tendon position on distal SO forces

ANOVA indicated a main effect of LG+PL proximal tendon position on SO distal total force (F_{SO}, $P < 0.001$) and an interaction effect between LG+PL proximal position and *group* ($P < 0.001$, Fig. 2A). In the controls, ΔF_{SO} with repositioning the proximal LG+PL tendon from $\boldsymbol{P^{A}_{REF}}-3$ mm to $\boldsymbol{P^{A}_{REF}}+3$ mm was 0.15 ± 0.14 N. This increased drastically to 0.47 ± 0.38 N and 0.80 ± 0.29 N for the 1 week and 2 weeks TI groups, respectively. In contrast, ΔF_{SO} was lower, but still significant for the AB groups (i.e., 0.07 ± 0.14 N and 0.09 ± 0.35 N for 1 and 2 weeks post-surgery, respectively). These results indicate that for each length increment of LG+PL proximally, more force was redirected from the distal tendons of LG+PL to the distal tendon of SO in the TI group compared to the other two groups. In contrast, the lower ΔF_{SO} in the AB group indicates a decrease of force transmitted between SO and LG+PL compared to control. Despite equal muscle masses (Table 1), F_{SO} at P_{REF} was substantially higher for the non-operated animals compared to the operated ones (up to 0.53 ± 0.20 N higher, or 38.8% of SO distal force at P_{REF} in controls), indicating a non-specific change in force-producing capacity of these muscles as a result of the mesh implantation surgery.

GEE analysis on $SLOPE_{SO}$ showed a significant interaction between the LG+PL proximal tendon position and TI group with respect to controls

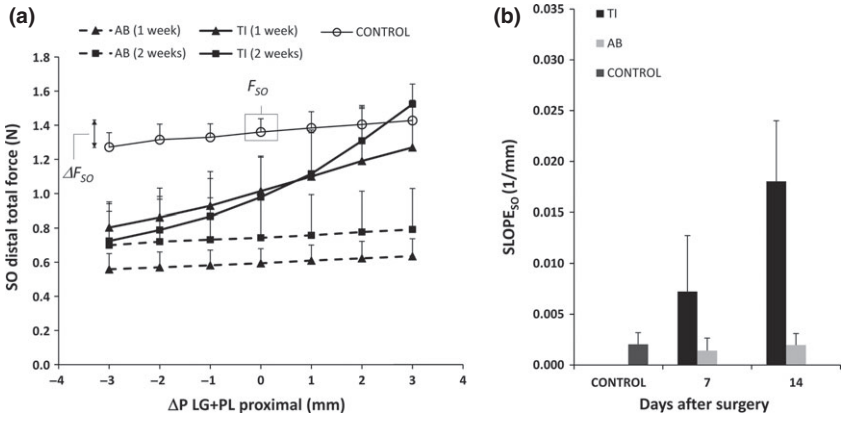

Fig. 2. Effects of lengthening LG+PL proximally on forces exerted at the distal tendon of soleus. (a) SO distal total force plotted as a function of the LG+PL proximal tendon position (ΔP_{LG+PL}) from −3 to +3 mm. ΔP_{LG+PL} is expressed as the deviation from the position corresponding to a 90° knee angle. Force values are not normalized (mean + SD, operated groups: $n = 16$, control: $n = 8$). Different lines correspond to control (solid-thick line), tissue-integrating mesh (TI, solid-thin line), and adhesion barrier (AB, dashed line) groups, 1 week (▲) or 2 weeks (■), after surgery. Single absolute SO distal force (F_{SO}) and range of force variation (ΔF_{SO}) with the full range of proximal LG+PL tendon displacement were reported on the control line for clarification. SO total force was on average considerably higher in the control group than in the operated animals ($P < 0.05$). (b) Range of mechanical interaction ($SLOPE_{SO}$, mean + SD) expressed as the maximal absolute change for normalized SO distal force within the imposed LG+PL proximal tendon positions range, ΔP = (−3; +3) mm from REF. Mechanical interaction significantly differed between the control and the increased-connectivity groups ($P < 0.05$) and a significant interaction effect was found between the manipulation type and the SO post-surgery recovery time ($P = 0.002$). No significant differences were observed between the non-operated group and the adhesion barrier groups ($P = 0.66$).

($P < 0.001$, Fig. 2B). In contrast, no interaction was found with the AB group vs control after normalization ($P = 0.66$). $SLOPE_{SO}$ was more than five times higher in the TI group (0.013 ± 0.008 mm^{-1}) with respect to control (0.002 ± 0.001 mm^{-1}). In addition, $SLOPE_{SO}$ was significantly different between TI-1 and TI-2 animals ($P = 0.002$), with the highest normalized force increase measured 2 weeks post-surgery (0.018 ± 0.006 mm^{-1}). Results from the normalized SO force show that the tissue-integrating mesh enhanced the mechanical interaction between LG+PL and SO compared to control, with the highest coupling occurring 2 weeks post-surgery.

Effects of LG+PL proximal tendon position on LG+PL proximal–distal force differences

Similar to SO distal force data, we found a main effect of proximal LG+PL tendon position on $\Delta F_{PROX\text{-}DIST}$ for all groups ($P < 0.001$), as well as an interaction effect between LG+PL tendon position and TI-AB manipulation (Fig. 3A, $P < 0.001$). In the control group, the $\Delta F_{PROX\text{-}DIST}$ ranged from -0.32 ± 0.11 N at $\boldsymbol{P^A_{REF}}-3$ mm to 0.06 ± 0.16 N at $\boldsymbol{P^A_{REF}}+3$ mm. Also for all other groups negative values were found at the most distal position ($\boldsymbol{P^A_{REF}}-3$ mm) and positive values at the most proximal one ($\boldsymbol{P^A_{REF}}+3$ mm), but with different magnitudes in the TI and AB groups. Note that any proximal–distal force difference indicates epimuscular myofascial force transmission. In particular, the negative $\Delta F_{PROX\text{-}DIST}$ measured at $\boldsymbol{P^A_{REF}}-3$ mm indicates net force transmission via epimuscular pathways to the distal LG+PL tendon; vice versa, the positive $\Delta F_{PROX\text{-}DIST}$ measured at $\boldsymbol{P^A_{REF}}+3$ mm indicates net force transmission to the proximal tendon of LG+PL.

GEE on $SLOPE_{LG+PL}$ showed an interaction effect between LG+PL proximal tendon position and TI group with respect to controls ($P < 0.001$, Fig. 3B), while no interaction was seen for the AB group vs control ($P = 0.83$). Compared to the control group ($SLOPE_{LG+PL} = 0.005 \pm 0.001$ mm^{-1}), $SLOPE_{LG+PL}$ was significantly higher in the TI-1 group (0.011 ± 0.006 mm^{-1}) and in the TI-2 group ($P = 0.004$; 0.023 ± 0.007 mm^{-1}), the latter being four times higher than in controls. The steeper increase in the normalized ΔF_{SO} (see previous paragraph) and $\Delta F_{PROX\text{-}DIST}$ indicates that after implantation of the tissue-integrating mesh, a higher percentage of force was attracted to the distal tendon of SO rather than to the distal tendon of LG+PL when LG+PL was lengthened proximally. The extent of such mechanical interaction increased between 1 and 2 weeks post-surgery.

Covariation of synergists' tendon force

A linear relationship between LG+PL proximal–distal force difference and SO distal force was found (Fig. 4). Regression analysis revealed a positive slope (model fit: $P < 0.001$) with a high degree of correlation for total forces in the TI-2 weeks group ($R = 0.98$) and lower, but still significant in the control, TI-1 week, and AB groups (Fig. 4, $R > 0.80$). Note that forces from LG+PL and SO were

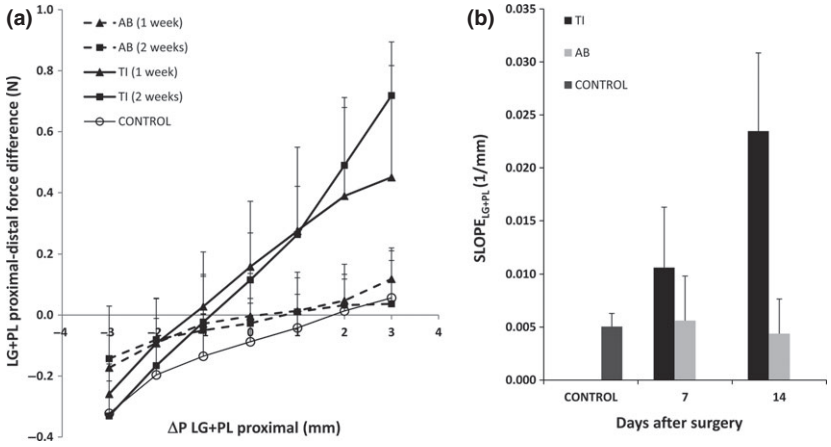

Fig. 3. Effects of lengthening LG+PL proximally on LG+PL proximal–distal tendon force difference. (a) Measured LG+PL proximal–distal total force difference ($\Delta F_{PROX\text{-}DIST}$) as a function of the position of the LG+PL proximal tendon (ΔP_{LG+PL}) from −3 to +3 mm (mean + SD, operated groups: $n = 16$, non-operated group: $n = 8$). ΔP_{LG+PL} is expressed as the deviation from the position corresponding to a 90° knee angle. Different lines correspond to control (solid-thick line), tissue-integrating mesh (TI, solid-thin line), and adhesion barrier (AB, dashed line) groups, 1 week (▲) or 2 weeks (■) after surgery. Average $\Delta F_{PROX\text{-}DIST}$ values differed significantly between operated and non-operated rats ($P < 0.05$). B) Range of mechanical interaction ($SLOPE_{PROX\text{-}DIST}$) expressed as the normalized maximal absolute change for $\Delta F_{PROX\text{-}DIST}$ within the imposed LG+PL proximal tendon positions, $\Delta P = (-3; +3)$ mm from REF. Mechanical interaction significantly differed between the control and the increased-connectivity groups ($P < 0.05$) as well as between 7 and 14 days post-surgery ($P = 0.004$). No significant differences were observed between the non-operated group and the adhesion barrier groups ($P = 0.83$).

expressed relative to the values of $\Delta F_{PROX\text{-}DIST}$ and F_{SO} measured at P_{REF}, respectively; therefore, the latter values were not included in the regression analysis. These data show that LG+PL and SO forces covaried with repositioning LG+PL proximal tendon, thus providing additional evidence of myofascial force transmission between these muscles.

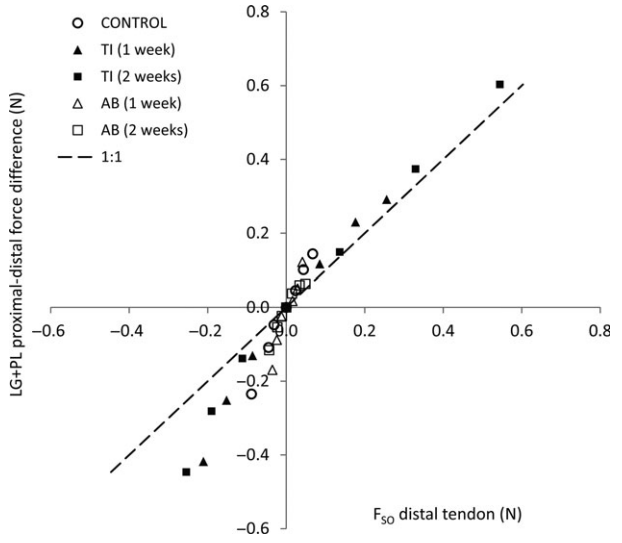

Fig. 4. Covariation of synergists' tendon force LG+PL. Proximal–distal tendon force (ΔF_{LG+PL}) was plotted as a function of SO distal tendon force (F_{SO}) for each step of SO/LG+PL relative displacement from $P_{REF} - 3$ to $P_{REF} + 3$ mm. Total forces (mean) are compared between the control group (CO, $n = 8$), the tissue-integrating mesh group (TI, $n = 8$), and the adhesion barrier group (AB, $n = 8$). Note that ΔF_{LG+PL} and F_{SO} are expressed relative to their values measured at P_{REF} ($\Delta P_{LG+PL} = 0$).

Effects of mesh implantation on passive muscle force

ANOVA indicated a main effect of LG+PL proximal position on SO distal passive forces ($P < 0.001$, Fig. 5A) and LG+PL proximal–distal passive force difference ($P < 0.001$, Fig. 5B). However, no interaction effect was found between LG+PL proximal position and the applied manipulation on SO passive force ($P = 0.560$), nor on the LG+PL proximal–distal passive force difference ($P = 0.212$). As the structure that is stiffest transmits most force, this indicates that the overall stiffness of the intermuscular pathways relative to that of the intramuscular pathways was unaltered in passive muscle conditions. Yet, ANOVA showed that the LG+PL proximal–distal passive force difference was changed in all the manipulated groups compared to control ($P < 0.001$). The LG+PL force difference curve was shifted up in a similar fashion ($P = 0.432$) and regardless of the type of manipulation for all operated animals compared to controls: passive forces at P_{REF} were on average 0.015 ± 0.004 N across the manipulation groups and -0.007 ± 0.012 N in controls (Fig. 5B), indicating a consistently higher proximal rather than distal passive force at LG+PL tendons. These results indicate differences in the mechanical effects of intermuscular linkages between active and passive state of the involved muscles. In addition, LG+PL neutral position (i.e., $\Delta F_{PROX\text{-}DIST} = 0$ N, see Fig. 5B) in controls (0.46 ± 1.52 mm) differed substantially from the value across all the manipulated groups, which ranged between $\boldsymbol{P^A_{REF}}-2.2$ mm and $\boldsymbol{P^A_{REF}}+0.5$ mm, while such neutral position was not affected by the manipulation type itself ($P = 0.694$). This substantial

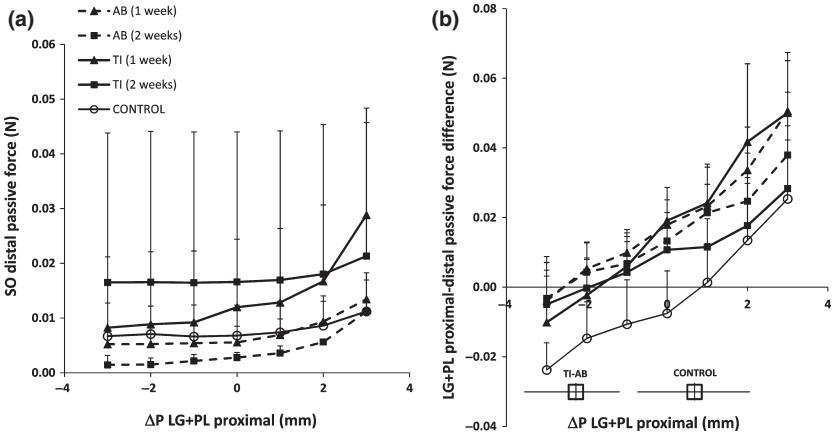

Fig. 5. Effects of intermuscular connectivity manipulation on passive forces of the synergistic group. Passive force measured at the distal tendon of SO (a) and LG+PL proximal–distal passive force difference (b) with increasing position of the LG+PL proximal tendon (ΔP_{LG+PL}) from −3 to +3 mm. ΔP_{LG+PL} is expressed as the deviation from the position corresponding to a 90° knee angle. Data points are averaged among animals that received the same connectivity manipulation procedure (solid line: tissue-integration mesh TI, dashed line: adhesion barrier mesh AB) and measured at the same time point (1 week: ▲ or 2 weeks ■, after surgery). No significant differences in passive SO force were found between groups ($P = 0.56$). LG+PL passive force difference resulted substantially higher in the altered connectivity condition, especially after 1 week after surgery ($P = 0.018$). LG+PL neutral position (mean ± SD, ⊕) was significantly different between intact and operated rats ($P < 0.001$).

difference in neutral positions indicates a change of configuration (i.e., length and angle) of the intermuscular connections after resection *in acute*.

Discussion

In this study, we showed that the mechanical interaction between rat ankle plantar flexors can be substantially altered by manipulating the connective tissue layers between them. In the control group, we found an increase of SO force with lengthening of the LG+PL proximal tendon (11.5% increase of SO force at P_{REF}). Because SO MTU length was kept constant, this force variation indicates mechanical interaction between SO and LG+PL muscles. Accordingly, the LG+PL proximal–distal tendon force difference also changed and these changes were highly correlated. These results provide evidence of the mechanical interaction between SO and LG+PL in the case of intact intermuscular connective tissues. Implantation of a tissue-integrating mesh resulted in a substantial increase in the extent of such interaction. These mechanical effects were evident already 1 week post-surgery and approximately doubled after 2 weeks, indicating a fast adaptation of myofascial connective tissues. In addition, no effects were observed after the application of an adhesion barrier aimed at reducing the extent of intermuscular interaction.

As no sham-operated group was used, possible non-specific effects of the connectivity manipulation surgery, such as pain-induced disuse, cannot be excluded. A sham surgery would involve, besides cutting the skin and compartmental fascia, also severing connective tissue linkages between SO and LG+PL. Because this will most likely lead to connective tissue remodeling at the interface between these muscles and, hence, altered intermuscular connectivity, such an approach was not deemed to be representative of the intact case. The results from the adhesion barrier group do provide some insight about possible sham effects. In this group, no differences in mechanical interaction between SO and LG+PL compared to controls were observed. This suggests that the enhanced interaction following implantation of the tissue-integrating mesh can be attributed to the experimental manipulation. However, we did find a shift upwards of the LG+PL passive force difference curve (Fig. 5B) as well as a decrease in muscle forces at reference length (Table 2) in all groups. These results suggest some specific effects of mesh implantation independent of mesh type. Therefore, our data must be interpreted considering possible confounders introduced by effects of surgery not related to the manipulation of intermuscular connectivity.

The active force reduction seen in both mesh-operated groups was independent of manipulation type, which suggests that such force drop was not directly related to intermuscular connectivity changes. Alternatively, the decrease of muscle force could be a consequence of shear-stress on the SO nerve induced by the mesh, although an opening was made in the mesh to accommodate the neurovascular tract of SO. Post-surgical unloading of the limb and muscle atrophy seems unlikely after comparing SO and LG+PL muscle masses of affected and unaffected limbs. However, growth of additional connective tissues on the surface of the muscle belly could mask muscle atrophy. These factors may explain the reduced force capacity of the synergistic muscle group in the operated rats compared to controls. To take this into account and allow for a fair comparison of mechanical interaction between groups, all forces were normalized to the sum of SO+LG+PL total force exerted distally (see methods).

Effects of increased intermuscular connectivity

Our data showed that an enhanced intermuscular connectivity between SO and LG+PL muscles caused a higher fraction of force to be redirected toward tendons of neighboring muscles. Epimuscular myofascial pathways are capable of transmitting substantial force between muscles (Huijing, 2009; Maas & Sandercock, 2010). Within a physiological range of muscle lengths and relative positions, however, only a limited fraction of muscle force is exchanged via epimuscular connective tissues (Bernabei et al., 2015). This fraction is determined by the stiffness ratio between the myofascial pathway and the myotendinous pathway. It has been hypothesized that epimuscular pathways become of greater importance after muscle or tendon trauma (Sandercock & Maas, 2009), when an increased stiffness of connective tissue linkages between muscles may occur. Although scar tissue formation has been reported at the muscle–tendon boundaries following muscle strain injury, tenotomy, and tendon transfer (Buller & Lewis, 1965; Nelson, 1969; Gold et al., 2004; Silder et al., 2008; Khanna et al., 2009; Maas & Huijing, 2012a,b), only few studies have investigated the mechanical effects of scar tissue. Riewald and Delp (1997) reported evidence of a residual knee extension moment of rectus femoris muscle after tendon transfer to the knee flexion side. It is conceivable that scar tissue formation and post-operative fascia remodeling provided a stiff pathway of force transmission to the neighboring knee extensors. Similar findings have been reported following flexor carpi ulnaris (FCU) tendon transfer in rat (Maas & Huijing, 2012a,b). By assessing force transmission from the transferred muscle, these experiments have shown that not all force generated within transferred FCU was transmitted to its distal tendon, but part of the force was redirected via scar tissue to other structures. Our and

previous studies indicate that the formation of additional connective tissue at the muscle–tendon boundary can have profound effects on muscular force transmission, thereby affecting the mechanical output of a muscle at the joint.

Mechanical interaction following adhesion barrier implant

Mechanical interaction between SO and LG+PL did not differ significantly in the AB group compared to controls. We hypothesized a reduction of mechanical interaction in this condition, as several previous studies have reported changes of intermuscular interaction following resection of connective tissues that served as pathways of force transmission (Smeulders et al., 2002; Maas et al., 2013). In this study, qualitative observations showed that the adhesion barrier did reduce the amount of connective tissue at the SO and LG+PL interface. However, connective tissue bundles, of which the specific location and firmness varied between animals, were frequently observed at the edges of the barrier, i.e., (a) branching out medially from the SO to the plantaris muscle belly, (b) laterally to the anterior crural compartmental fascia; (c) distally attaching to the Achilles tendon and the biceps femoris fascia. Qualitative observations of the progression of tissue-adhesion recurrence were in agreement with previous studies using adhesion barriers similar to the ones used in this study (Novitsky et al., 2007; Rodríguez et al., 2011). In the present experiment, such a variety of anchoring sites for the AB implant during recovery may be explained by the fact that the mesh was not sutured to the muscle belly surface. Such a procedure was applied to prevent the formation of unwanted linkages. Besides newly formed connective tissue linkages, the neurovascular tract, a connective tissue structure embedding the blood vessels and nerves for SO muscle, was still intact. Substantial mechanical interaction between the anterior crural muscles of the rat with only the neurovascular tract intact has been reported (Maas et al., 2005; Yucesoy et al., 2006). We conclude that the inability to reduce the mechanical coupling between SO and LG+PL with the adhesion barrier can be explained by force transmission via newly formed connective tissue linkages and the neurovascular tract of SO.

Different effects of altered intermuscular connectivity between active and passive muscle

Unlike during active muscle contraction, the transmission of passive force per unit of relative displacement between passive SO and LG+PL muscles was not significantly affected by implantation of the tissue-integrating mesh. This finding shows that changes in the connective tissue layer between synergists are not expressed equally in passive and active muscle. Such a discrepancy has previously been observed in animal studies investigating effects of disrupting different connective tissues. Compartmental fasciotomy (Smeulders et al., 2002) and progressive muscle belly dissection (Maas & Huijing, 2012a,b) resulted in substantial changes of the length-active force characteristics, while length-passive force characteristics were not affected. A main difference between passive and active conditions is the stiffness of the muscle belly. In fact, when the relative position is changed between passive muscles, compliant intramuscular structures could fully absorb the resulting shear strain and, hence, the myofascial connections may not experience any strain. Conversely, activating the muscle fibers will increase the stiffness of the muscle belly. As a consequence, less deformation of intramuscular structures and, thus, greater lengthening of myofascial connections with the same muscle relative displacement are expected. We conclude that consequences of scar tissue formation for intermuscular transmission of force are dependent on whether a muscle and its neighboring synergist are in an active or a passive state. As previously noted (Smeulders et al., 2002), this has implications for surgeon's intraoperative estimation of muscle function, which is routinely carried out only by assessing forces of passive muscles.

Perspectives

Muscle injuries are among the most common sport-related injuries, with more than 90% being caused either by contusion or excessive strain of the muscle (Garrett, 1996; Ekstrand et al., 2011). Shearing type of muscle injuries are associated with rupture of myofibers and surrounding connective tissue framework with subsequent formation of scar tissue (Kääriäinen et al., 2000). The results of the present study show that an increased intermuscular connectivity alters force transmission within a muscle group. In case of muscle injury, abnormal connective tissues pathways may redirect part of the force to intact tissues bypassing the damaged area (Maas & Sandercock, 2010). Such spatial dissipation of contractile force may prevent high local stresses (Bojsen-Moller et al., 2010) and facilitate recovery of the damaged area as well as restore function before the healing is complete. On the other hand, scar tissue has also been associated with a reduction of the overall muscle belly displacement and a localized increase of tissue strain (Silder et al., 2008), which may potentially extend the damage to neighboring muscles. Besides muscle–tendon injuries, similar mechanical effects of scar tissue may be expected following orthopedic surgical interventions involving disruption of muscle or connective tissues (e.g., fasciotomy, aponeurotomy, and tenotomy).

Key words: Muscle injury, myofascial force transmission, scar tissue, stiffness, soleus, gastrocnemius, synergists.

Acknowledgements

We thank Guus C. Baan for contributing to this article with the design and development of a 3D model of the rat lower limb muscles.

Funding

This study was supported by Division for Earth and Life Sciences of the Netherlands Organization for Scientific Research to H. Maas [864-10-011].

Disclosures

No conflicts of interest, financial, or otherwise, are declared by the authors.

References

Bauman JM, Chang YH. High-speed X-ray video demonstrates significant skin movement errors with standard optical kinematics during rat locomotion. J Neurosci Methods 2010: 1: 18–24.

Bernabei M, van Dieën JH, Baan GC, Maas H. Significant mechanical interactions at physiological lengths and relative positions of rat plantar flexors. J Appl Physiol 2015: 118: 427–436.

Bojsen-Moller J, Schwartz S, Kalliokoski KK, Finni T, Magnusson SP. Intermuscular force transmission between human plantarflexor muscles in vivo. J Appl Physiol 2010: 6: 1608–1618.

Buller AJ, Lewis DM. Some observation on the effects of tenotomy in the rabbit. J Physiol 1965: 178: 326–342.

Canu MH, Garnier C. A 3D analysis of fore- and hindlimb motion during overground and ladder walking: comparison of control and unloaded rats. Exp Neurol 2009: 1: 98–108.

Ekstrand J, Hägglund M, Waldén M. Epidemiology of muscle injuries in professional football (soccer). Am J Sports Med 2011: 6: 1226–1232.

Garrett WE. Muscle strain injuries. Am J Sports Med 1996: 6(Suppl): S2–S8.

Garrett WEJ, Nikolaou PK, Ribbeck BM, Glisson RR, Seaber AV. The effect of muscle architecture on the biomechanical failure properties of skeletal muscle under passive extension. Am J Sports Med 1988: 1: 7–12.

Gillis GB, Biewener AA. Hindlimb muscle function in relation to speed and gait: in vivo patterns of strain and activation in a hip and knee extensor of the rat (Rattus norvegicus). J Exp Biol 2001: 15: 2717–2731.

Gold GE, Asakawa DS, Blemker SS, Delp SL. Magnetic resonance imaging findings after rectus femoris transfer surgery. Skeletal Radiol 2004: 1: 34–40.

Greene EC. Anatomy of the Rat. In: Transactions of the American Philosophical Society, New Ser. Vol. 27. American Philosophical Society 1935: ii-vii + ix-xi + 1–370.

Huijing PA. Epimuscular myofascial force transmission: a historical review and implications for new research. International Society of Biomechanics Muybridge Award Lecture, Taipei, 2007. J Biomech 2009: 1: 9–21.

Huijing PA, Voermans NC, Baan GC, Busé TE, Van Engelen BGM. de Haan A. Muscle characteristics and altered myofascial force transmission in tenascin-X-deficient mice, a mouse model of Ehlers-Danlos syndrome 2010: 18: 986–995.

Huijing PA, Yaman A, Ozturk C, Yucesoy CA. Effects of knee joint angle on global and local strains within human triceps surae muscle: MRI analysis indicating in vivo myofascial force transmission between synergistic muscles. Surg Radiol Anat 2011: 10: 869–879.

Johnson WL, Jindrich DL, Roy RR, Reggie Edgerton V. A three-dimensional model of the rat hindlimb: musculoskeletal geometry and muscle moment arms. J Biomech 2008: 41: 610–619.

Kääriäinen M, Järvinen T, Järvinen M, Rantanen J, Kalimo H. Relation between myofibers and connective tissue during muscle injury repair. Scand J Med Sci Sports 2000: 10: 332–337.

Khanna A, Friel M, Gougoulias N, Longo UG, Maffulli N. Prevention of adhesions in surgery of the flexor tendons of the hand: what is the evidence? Br Med Bull 2009: 1: 85–109.

Kreulen M, Smeulders MJC, Hage JJ, Huijing PA. Biomechanical effects of dissecting flexor carpi ulnaris. J Bone Joint Surg [Br] 2003: 6: 856–859.

Maas H, Baan GC, Huijing PA. Dissection of a single rat muscle-tendon complex changes joint moments exerted by neighboring muscles: implications for invasive surgical interventions. PLoS ONE 2013: 8: e73510.

Maas H, Baan GC, Huijing PA, Yucesoy CA, Koopman BHFJM, Grootenboer HJ. The Relative Position of EDL Muscle Affects the Length of Sarcomeres Within Muscle Fibers: Experimental Results and Finite-Element Modeling. J Biomech Eng 2003: 125: 745–753.

Maas H, Huijing PA. Effects of tendon and muscle belly dissection on muscular force transmission following tendon transfer in the rat. J Biomech 2012a: 2: 289–296.

Maas H, Huijing PA. Mechanical effect of rat flexor carpi ulnaris muscle after tendon transfer: does it generate a wrist extension moment? J Appl Physiol 2012b: 4: 607–614.

Maas H, Meijer HJM, Huijing PA. Intermuscular interaction between synergists in rat originates from both intermuscular and extramuscular myofascial force transmission. Cells Tissues Organs 2005: 1: 38–50.

Maas H, Sandercock TG. Force transmission between synergistic skeletal muscles through connective tissue linkages. J Biomed Biotechnol 2010: 2010: 575672.

Magnuson DS, Smith RR, Brown EH, Enzmann G, Angeli C, Quesada PM, Burke D. Swimming as a model of task-specific locomotor retraining after spinal cord injury in the rat. Neurorehabil Neural Repair 2009: 6: 535–545.

Nelson PG. Functional consequences of tenotomy in hind limb muscles of the cat. J Physiol 1969: 2: 321–333.

Nikolaou PK, MacDonald BL, Glisson RR, Seaber AV, Garrett WE. Biomechanical and histological evaluation of muscle after controlled strain injury. Am J Sports Med 1986: 1: 9–14.

Novitsky YW, Harrell AG, Cristiano JA, Paton BL, Norton HJ, Peindl RD, Kercher KW, Heniford BT. Comparative evaluation of adhesion formation, strength of ingrowth, and textile properties of prosthetic

meshes after long-term intra-abdominal implantation in a rabbit. J Surg Res 2007: 1: 6–11.
Riewald SA, Delp SL. The action of the rectus femoris muscle following distal tendon transfer: does it generate knee flexion moment? Dev Med Child Neurol 1997: 39: 99–105.
Rodríguez M, Pascual G, Sotomayor S, Pérez-Köhler B, Cifuentes A, Bellón JM. Chemical adhesion barriers: do they affect the intraperitoneal behavior of a composite mesh? J Invest Surg 2011: 3: 115–122.
Sandercock TG, Maas H. Force summation between muscles: are muscles independent actuators? Med Sci Sports Exerc 2009: 1: 184–190.
Silder A, Heiderscheit BC, Thelen DG, Enright T, Tuite MJ. MR observations of long-term musculotendon remodeling following a hamstring strain injury. Skeletal Radiol 2008: 12: 1101–1109.
Silder A, Reeder SB, Thelen DG. The influence of prior hamstring injury on lengthening muscle tissue mechanics. J Biomech 2010: 12: 2254–2260.
Smeulders MJC, Kreulen M. Myofascial force transmission and tendon transfer for patients suffering from spastic paresis: a review and some new observations. J Electromyogr Kinesiol 2007: 6: 644–656.
Smeulders MJ, Kreulen M, Hage JJ, Baan GC, Huijing PA. Progressive surgical dissection for tendon transposition affects length-force characteristics of rat flexor carpi ulnaris muscle. J Orthop Res 2002: 4: 863–868.
Smeulders MJC, Kreulen M, Hage JJ, Huijing PA, van der Horst CMAM. Intraoperative measurement of force-length relationship of human forearm muscle. Clin Orthop Relat Res 2004: 418: 237–241.
Smeulders MJC, Kreulen M, Hage JJ, Huijing PA, van der Horst CMAM. Spastic muscle properties are affected by length changes of adjacent structures. Muscle Nerve 2005: 2: 208–215.
Tian M, Herbert RD, Hoang P, Gandevia SC, Bilston LE. Myofascial force transmission between the human soleus and gastrocnemius muscles during passive knee motion. J Appl Physiol 2012: 4: 517–523.
Yaman A, Ozturk C, Huijing PA, Yucesoy CA. Magnetic resonance imaging assessment of mechanical interactions between human lower leg muscles in vivo. J Biomech Eng 2013: 9: 91003.
Yucesoy CA, Huijing PA. Substantial effects of epimuscular myofascial force transmission on muscular mechanics have major implications on spastic muscle and remedial surgery. J Electromyogr Kinesiol 2007: 6: 664–679.
Yucesoy CA, Maas H, Koopman BHFJM, Grootenboer HJ, Huijing PA. Mechanisms causing effects of muscle position on proximo-distal muscle force differences in extra-muscular myofascial force transmission. Med Eng Phys 2006: 3: 214–226.